International Journal of Scientific Engineering and Applied Science (IJSEAS) – Volume-7, Issue-5, May 2021
ISSN: 2395-3470
www.ijseas.com

Design Optimization of a Cross-Flow Micro Hydropower Turbine Using CFD Analysis

Yusuf Yakubu[1], F. O. Anafi[2], G. Y. Pam[3], C. O. Folayan[4] and Young-Ho Lee[5]

[1] Dept. of Mechanical Engineering, Ahmadu Bello University, Zaria, Nigeria

[2] Dept. of Mechanical Engineering, Ahmadu Bello University, Zaria, Nigeria

[3] Dept. of Mechanical Engineering, Ahmadu Bello University, Zaria, Nigeria

[4] Dept. of Mechanical Engineering, Ahmadu Bello University, Zaria, Nigeria

[5] Division of Mechanical and Information Engineering, Korea Maritime and Ocean University, Busan, Korea
(Corresponding Author)

Abstract

The availability of robust computer technologies and design developments were utilized in carrying out CFD based study on the design, performance characteristics, flow analyses and design optimization of a simple cross flow turbine. The CFX-Pre settings include two phase (air & water at 25°C) steady state with shear stress turbulence (SST) model in the commercial CFD code ANSYS CFX 13.0. The design parameters include 5m head, 0.07-0.08 m^3/s flow rates and 250-400 rpm rotational speeds. Turbine parameters such as nozzle arc angle, angle of attack, nozzle width ratio, blade numbers, blade angles, diameter ratio, blade radius and casing width were analysed. In addition, the use of standard pipe strips of various diameters as blades were simulated. The 72mm diameter pipe strip used when inlet angle tilted at 28^o, outlet angle of 92^o, diameter ratio of 0.69 and 26 blades was found to be optimum with gained of 7.1% efficiency; the modification of nozzle shape improved the efficiency by 7.9%. Extension of the turbine casing around the nozzle tip improved the efficiency by 1.9%.

Keywords: *Crossflow turbine, Nozzle, Runner-blade, Ansys-CFX, Diameter-ratio, Turbine-casing.*

1. Introduction

Cross flow hydropower turbine has the advantage of low cost of manufacture, operation, maintenance and good performance at part flow condition (N. H. Pereira *et al.*, 2014). However, it has low peak efficiency compared to Pelton and Kaplan turbines (Adhikari *et al.*, 2018). Therefore, the various effort to improve its performance, since it is the most suitable turbine for harnessing small hydropower power especially in the rural communities of developing countries (Dametew, 2016).

Efficiency of hydropower turbine relates its hydraulic power to its torque power. The performance of the turbine is ascertained based on this relation. In general, efficiency indicates the percentage of the input power that is converted to rotational which can be used to drive generator or any mechanical equipment. This is given by the equation 1 (Tongco, 1988);

$$\eta = \frac{\tau_t \omega}{\gamma Q H_n} \quad (1)$$

According to Mockmore *et al.* (1949), maximum efficiency can be written as in equation 2, and to obtain the highest mechanical efficiency, the entrance angle α should be as small as possible. they considered value of α to be 16^o while C and φ to 0.98 each, given a theoretical efficiency of 87.8%.

$$\eta = \frac{1}{2} * C^2 * (1 + \varphi) * (\cos\alpha_1{}^2) \quad (2)$$

However, Oliy *et al.* (2017) found out in a theoretical and numerical studies that entrance angle of 18^o gives the maximum efficiency at full gate opening. Totapally *et al.* (1994) noted that for the maximum efficiency to be a function of angle of attack as indicated, assumptions made in the analysis (equation 2.2) should be ideally satisfied. Otherwise, it would be valid for single operation only. Tiwari *et al.* (2017) shows that radius of curvature and diameter ratio influence on the turbine efficiency are not too significant. His findings were collaborated by that of Olgun (1998) and Ceballos *et al.* (2017) whose indicated difference of only 3% and 3.2% respectively in efficiency, for varying the diameter ratios.

According to Khosrowpanah *et al.* (1988) and Totapally *et al.* (1994), too many blades increase the runner weight and reduced flow passages while few numbers of blades cause higher losses due to flow separation. Peláez Restrepo (2014) and Desai *et al.* (1994) in different studies of crossflow turbine observed that runners with greater number of blades performs better than those with fewer blades. Pokhrel (2017) found out that runner with 8 blades performed better than that with 12 blades. Joshi *et al.* (1995) compare the effect of changing the blade number on heads using different nozzles. They observed

that for smaller entry arc (26^o), the increased in efficiency with increased supply head is more pronounced for large blade numbers than for the smaller values. for larger entry arc (36^o), the maximum efficiency decreases with increased head. They further observed that a runner of a given dimension has an optimal flow rate at which the efficiency is maximum. Results of these various studies signifies that optimum number of blades for effective performance of a cross-flow turbine depends on several parameters.

Nozzle should be designed in such a way that pressure is fully converted to velocity before the flow entered the runner for better efficiency (Adhikari, 2016; N. C. Pereira *et al.*, 1996). Good nozzle angle designed ensures stable transition of the flow especially for the first stage (Soenoko, 2016). Totapally *et al.* (1994) observed that a compromise has to be reach on the selection of nozzle throat width ratio, which depends on the value of nozzle throat width (S_o). According to them, higher value of S_o would be advantageous due to the fact that the losses due to filling and emptying the runner would be small. However, the value of the angle of attack at the outer filaments of the jet would vary considerably from the designed value. Nakase (1982) formulated relationship for nozzle throat width ratio shown in equation 3 and revealed value of 0.26 as most suitable.

$$\frac{S_o}{R_1\theta} = \sin\alpha = T_R \qquad (3)$$

Fukutomi *et al.* (1995) observed that large value of T_R results in large value of flow angle, and an increase in flow angle results in shock losses at the blade inlet. The exit pressure also increases with increase value of T_R. Desai *et al.* (1994) recommended the most efficient nozzle as the one having angle of attack of 24^o, entry arc of 90^o and throat width ratio of 0.41. Djoko Sutikno *et al.* (2019) also observed that turbine performance decreases with increased nozzle arc from 90-120^o and concluded that the turbine efficiency is influenced by the magnitude of the entry arc and the rotational speed. Findings made in a related studies (Djoko; Sutikno *et al.*, 2019), observed that the characteristics of the turbine changes with nozzle entry arc, mass flowrate and head. They also observed that nozzle made with roof curvature having its radius centered on the shaft axis performed better. Another feature exhibited by cross flow turbine which is not common with impulse turbine is having a considerable amount of static pressure at the nozzle outlet (N. Acharya *et al.*, 2015; Fukutomi *et al.*, 1995; Walseth, 2009). Joshi *et al.* (1995) found out that this residual static pressure at the nozzle exit increases with increased supply head. Choi *et al.* (2012) reduced the amount of static pressure at the nozzle exit through optimization of the nozzle shape to a narrow and contracting passage. Though, there is a limit to narrowing the shape of the semi spiral casing of the nozzle for optimum performance (Benišek *et al.*, 2005).

CFD is a means of solving fluid flows by numerical techniques with the aid of computer (R. Acharya, 2016). Calculations are based upon the fundamental governing equations of fluid dynamics: the conservation of mass, momentum and energy (Anderson *et al.*, 2013). These equations combined to form the Navier-Stokes equations, which are set of partial differential equations (PDEs) that cannot be solved analytically except in a limited number of cases (Hu, 2012; Khare *et al.*, 2010). The fluid equations are replaced by discrete approximations at grid points that must be close enough for the solution to be independent of the grid point spacing (Anderson *et al.*, 2013). Iovănel *et al.* (2019) compared the performance of different turbulent models in both steady and unsteady numerical analysis of Kaplan turbine and found out that K-epsilon and SST-CC produced most accurate results. K-epsilon performs poorly in simulating complex flow where large pressure gradient, strong streamline curvature and separations are involved (Gu *et al.*, 2014). However, SST with automatic wall function and in combination of a model for transition from laminar to turbulent shows superiority over other models when implemented in ANSYS CFX (Orso *et al.*, 2020), and is also proven to show less sensitivity to variation of grid sizes (Menter *et al.*, 2003). Adanta *et al.* (2018) observed that flow streams expanded after hitting the blades of a crossflow turbine, which resulted in pressure increased with resulting recirculation. In such situation, SST model would be the preferable model for simulating the flows (Adanta *et al.*, 2019). This is because it has been proven to give accurate results in cases involving adverse pressure gradient flows and where separations occur (Bijukchhe, 2012). SST turbulent model was chosen for this work except where comparisons were made with other numerical models.

2. METHODOLOGY

2.1 Numerical Method

The fluid domain was CAD modelled with Unigraphics NX6 developed by SEIMENS Incorporation. The models designed were directly imported to the grid generation software ICEM CFD. The meshing of the fluid domain was divided in three standalone meshing components as shown on Figure 3.3, two for the stationary domains and one for the rotating domain. The nozzle been the most complicated part was meshed with Tetra-Delaunay with inflated prism layers around the inlet and outlet boundaries as shown in Figure 1. The rotor blades and internal fluid were meshed with Hexahedral meshing technique with O-grid around the curve surfaces. The reason behind the use of prism layers and O-grid is to capture the boundary layer flows correctly as indicated in Figures 2 and 3.

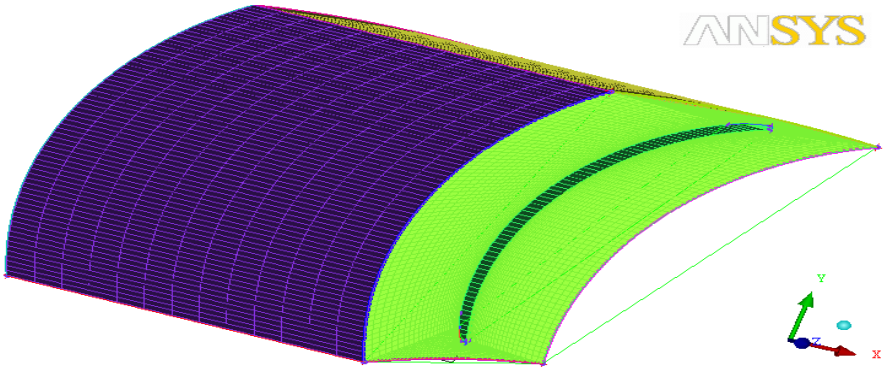

Figure 1: Meshed Runner Blade (Hexa) in ANSYS ICEM CFD

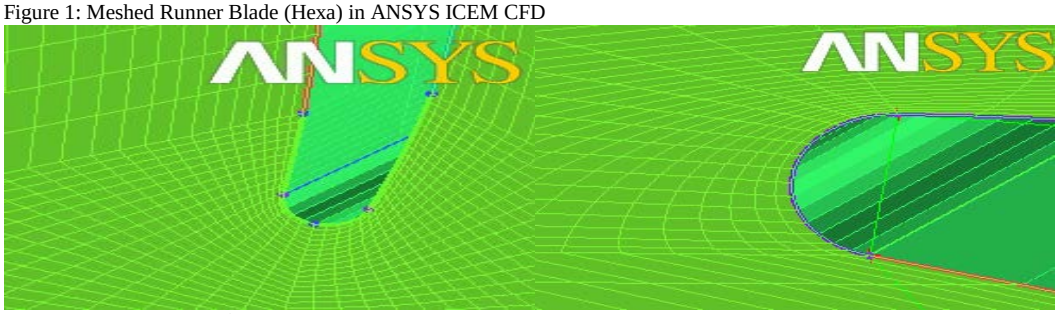

Figure 2: Concentration of mesh at the boundary layer

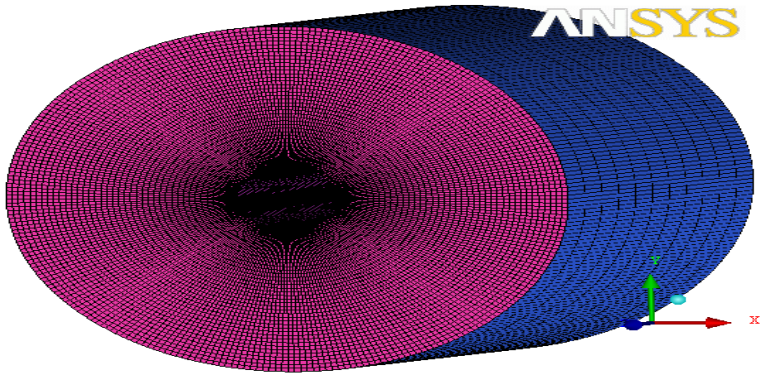

Figure 3: Meshing of Runner Fluid (Hexa)

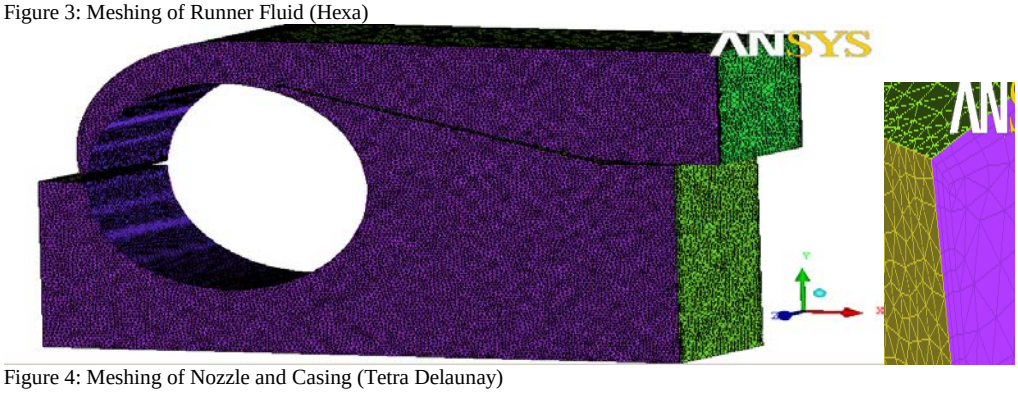

Figure 4: Meshing of Nozzle and Casing (Tetra Delaunay)

2.2 Procedure

The steady state was selected for all simulation, high resolution advection scheme and first order turbulent numeric options with maximum iteration of 500 were chosen. The physical time scale of 1/ω and conservation criteria residual target of 1 x

10^{-5} were selected. The conservation target of 0.01 was set for all the simulation. The reference pressure was set to 1*atm* and homogeneous model was chosen for all the domains. The standard free surface model was chosen because the air and water interface were considered distinct. The surface tension coefficient was set manually to 0.075 *Nm*−1. SST turbulence model was selected. Heat transfer was neglected in all the cases run, although there is a small temperature difference before and after the energy conversion in the runner. For initial conditions, the cartesian velocity components were set to zero and the volume fraction of air and water were set to 0 and 1 respectively for the Nozzle, Runner and Internal Fluid domains.
All the walls mass and momentum were set to "no slip condition". The inlet boundary was set to "Bulk Mass Flow rate" and the outlet boundary was set to "opening" and mass and momentum option was set to "opening pressure and dirn" and relative pressure to zero. High Resolution, First Order, was chosen and the minimum iteration was set to 1 and maximum was set to 500. The residual type RMS (root mean square) was chosen with a residual target of 1.0×10^{-5}.
The main output of the simulation are the inlet and outlet pressures of the turbine and torque transferred by the blades. Expressions of these outputs were added and logged in the monitored output to monitor convergence.

3 Results and analysis

The detailed results of optimal shapes and values for geometrical and non-geometrical parameters are presented. the geometrical parameters include nozzle shape (arc radius and length, angle of attack and nozzle width), Blade shape (diameter ratio, blade angles, radius of curvature, blade thickness, blade number and shape of blade tip) and casing shape were simulated. The non-geometrical parameters include head, flow rate and rotational speed, Results of the variation of the above parameters in terms of inlet pressure, outlet pressure and torque were presented.

3.1 Base design analysis

Figures 3.1 to 3.3 show the Performance curves of the baseline turbine by variation of the discharge between 0.07 m^3/s and 0.08 m^3/s at interval of 0.005 m^3/s and at optimum speed of 350 rpm. The variation of flow rate from the calculated value improved the efficiency by 1.2%.

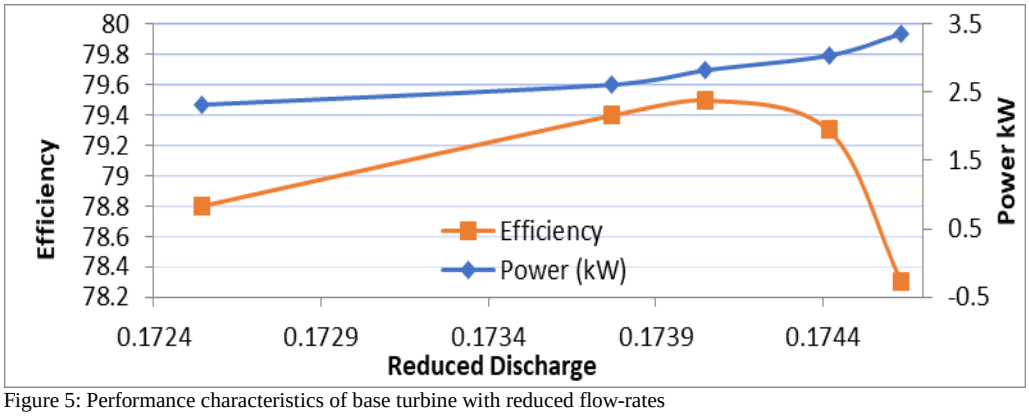

Figure 5: Performance characteristics of base turbine with reduced flow-rates

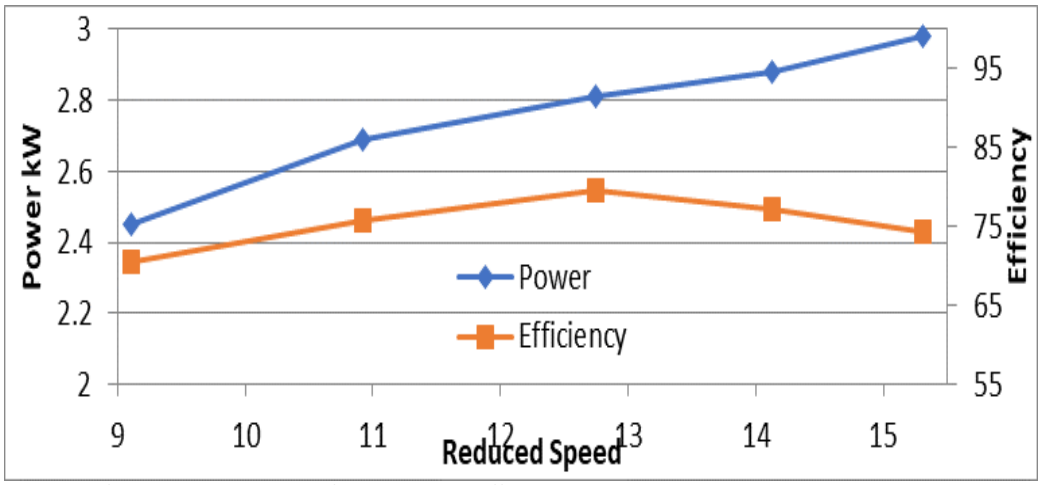

Fig. 3.2 Performance characteristics of base turbine at different rpm

Fig 3.3: Performance characteristics of base turbine with K-E and SST turbulent models against variable speed

3.2 Performance Optimization Analysis

Nozzle admission arc

The nozzle entry arc was varied at interval of 2.5^{o} and simulated at optimized flow rate of 75litre per second and rotational speed of 350 rpm. Table 4.4 contained the values of shaft power and efficiency and Figure 3.4 shows the Performance curves of the turbine by variation of the nozzle admission arc. The performance of the turbines increases with an increased in nozzle entry arc as observed by Joshi *et al.* (1995).

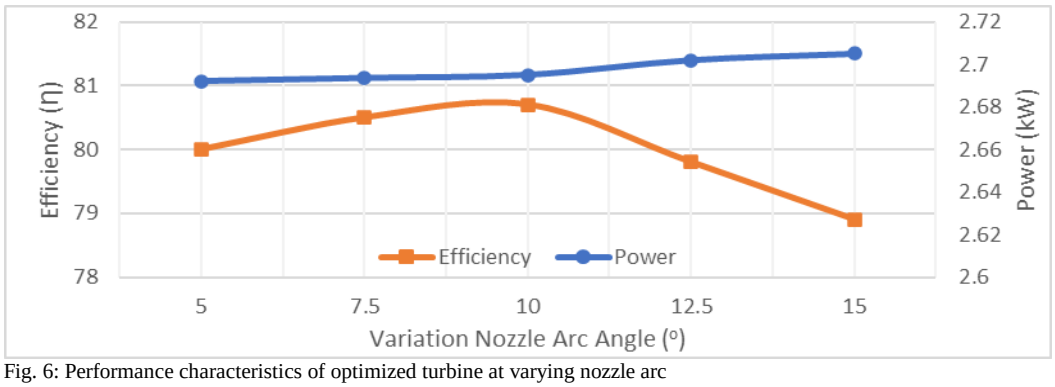

Fig. 6: Performance characteristics of optimized turbine at varying nozzle arc

Nozzle angle of attack

The nozzle angle of attack was varied at 14°, 15°,16°, 17° and 18° and simulated with optimized flow rate of 75litre per second and rotational speed of 350 rpm.

Figure 3.4 shows the Performance curves of the turbine with variation of the angle of attack. The efficiency increases marginally from 80.5% at angle 14° to the peak of 80.7% at 16° and begun to fall down to 78.9% at 18°. The shaft power decreased by 16 watts.

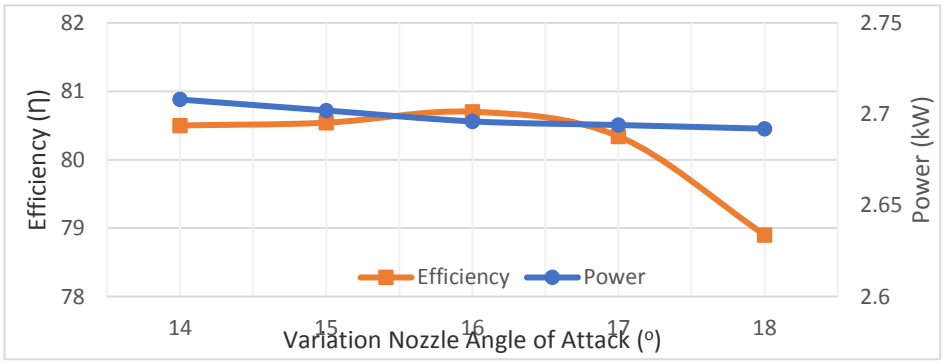

Fig. 7: Performance characteristics of optimized turbine at varying nozzle angle of attack

Comparing the velocity contours in Figure 3.7, it can be seen that water sticks on the blades when the angle increases to 18°, therefore retarding the runner speed and reduces available flow to the second stage power. The maximum velocity of the water decreases when the angle increased from 16° to 18°.

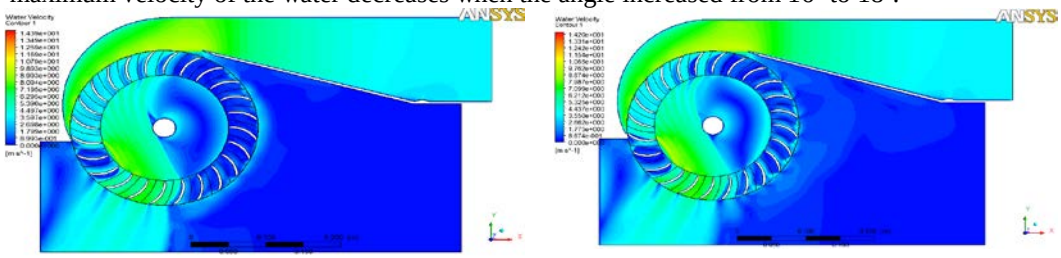

Figure 8: Comparison of Velocity contour by variation of Nozzle angle of attack between 16° (Left) and 18° (Right)

Nozzle width optimization

The nozzle width was varied between 160mm and 170mm at 2.5mm interval and simulated with optimized flow rate of 75litre per second and rotational speed of 350 rpm.

Figure 9 shows the Performance curves of the turbine with the variation of nozzle width.

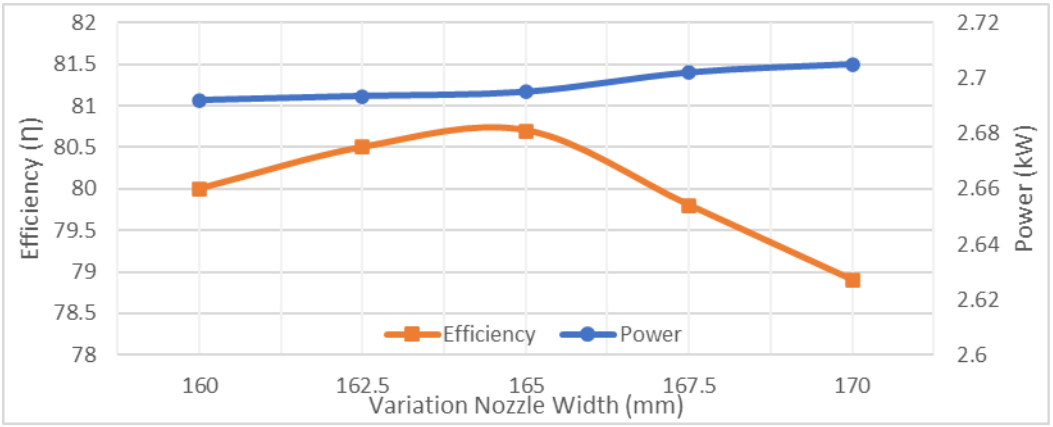

Fig. 9: Performance characteristics of optimized turbine at varying nozzle width

Fig. 10 shows the comparison of velocity contours of the turbine by extending the nozzle width from 160mm to 170mm at interval of 5mm. There was drop in inlet pressure at constant flow when the width of the nozzle was increased from 160mm to 170mm at 5mm interval. However, the efficiency improved significantly. An efficiency increased by 6.4% which was consistent with the observation of Sammartano *et al*. (2013) . Both the velocity and water volume ratio contours illustrated how chaotic the water leaving the turbine was in the case of 160mm width nozzle; which justified the major loss in efficiency.

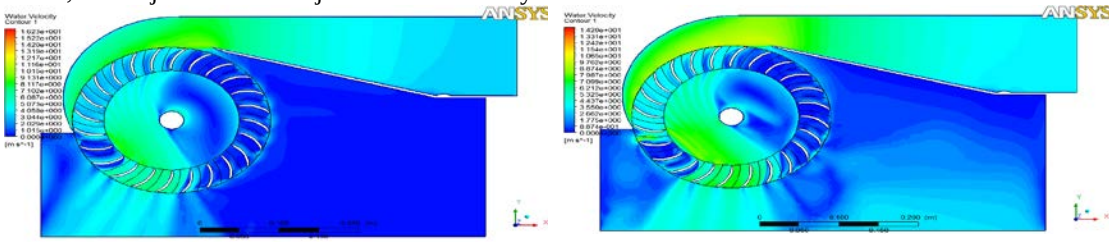

Figure 10: Comparison of Performance between B170 and B160 Nozzle Design @ 75L and 350rpm

Blade radius

The blade radius was varied based on the standard pipe sizes available in the market and their performances were simulated using optimized flow rate of 75litre per second and rotational speed of 350 rpm. Figure 4.25 shows the Performance curves of the turbine by variation of the blade radius.

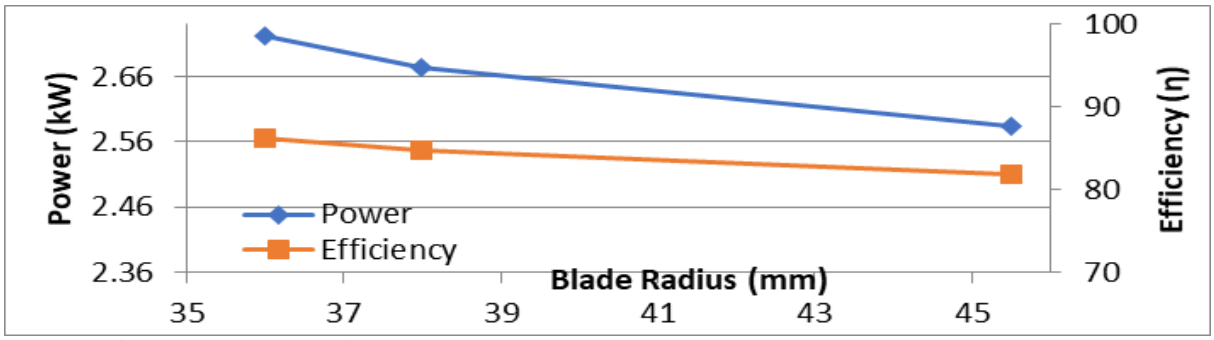

Fig. 11: Performance characteristics of optimized turbine at varying runner blade radius

There was significant increase in both the power output and the efficiency when the radius of curvature was varied between 36mm and 45.5mm. An additional power of 443W and efficiency of 5% were obtained by this variation.

Blade thickness

The blade thickness was varied based on the sizes available in the market and their performances were simulated using optimized flow rate of 75litre per second and rotational speed of 350 rpm. Figure 4.12 shows the Performance curves of the turbine by variation of the blade thickness.

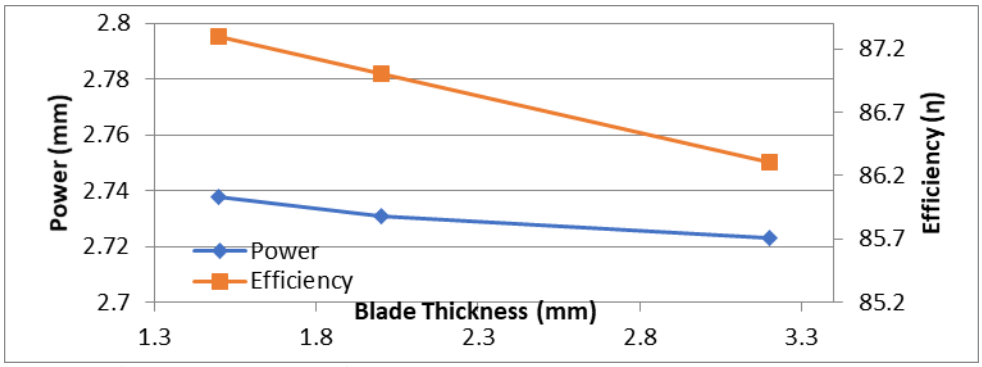

Fig. 12: Performance characteristics of optimized turbine with varying runner blade thickness

An additional output power of 15W and efficiency of 1% were obtained with this variation.

Blade diameter ratio optimization

The blade diameter ratio was varied between 0.66 and 0.71, their performances were simulated using optimized flow rate of 75litre per second and rotational speed of 350 rpm. Figure 13 shows the Performance curves of the turbine by variation of the blade diameter ratio.

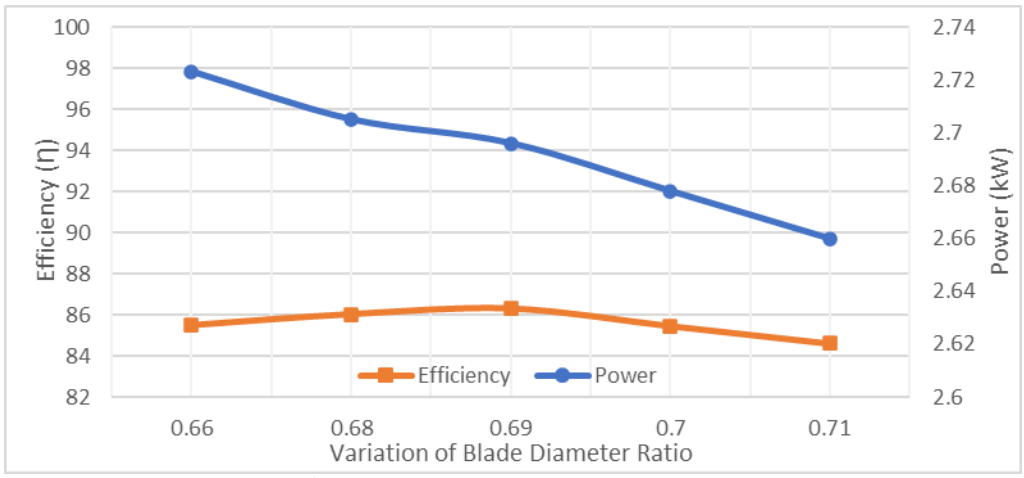

Figure 13: Water Velocity Contour for baseline design at 300 rpm and 75 litre/s

comparison of pressure contours, velocity contours, water volume fraction contours, and velocity vector of the turbine by extending the entry arc with additional 5 to 15 degrees. There was 27W dropped in output power but 0.8% increase in efficiency with the variation of runner diameter ratio.

Blade number optimization

The blade number was varied between 24 and 27, their performances were simulated using optimized flow rate of 75litre per second and rotational speed of 350 rpm. Figure 14 shows the Performance curves of the turbine by variation of the blade number.

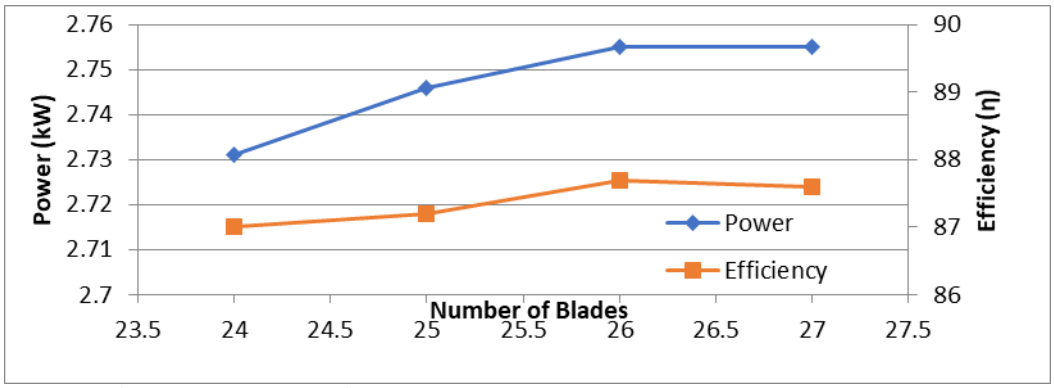

Fig. 14: Performance characteristics of optimized turbine with varying blade number

Figure 15 shows the comparison of velocity contours of the turbine by varying the number of blades. Increasing the number of blades from 24 to 27 produced 24W additional power and 0.7% marginal increased in efficiency. This observation was also made by Mani *et al.* (2016) Sammartano *et al.* (2013), and Tongco (1988).

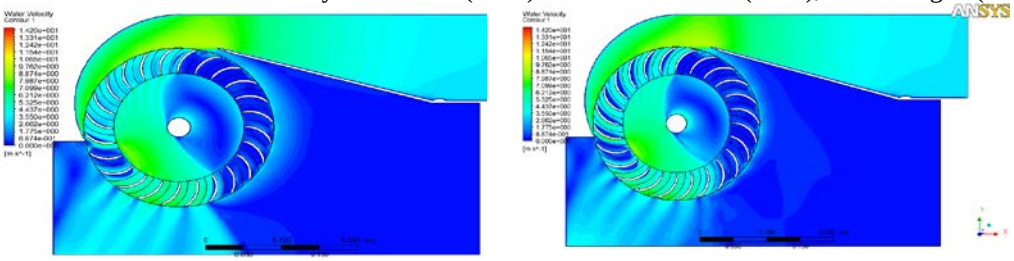

Fig. 15: Comparison of Performance between Blade Number of 24 and 27 @ 75L and 350rpm

Blade entry and exit angles

The blade entry and exit angles were varied between 28.1°/87.9° and 24.1°/91.9°, their performances were simulated using optimized flow rate of 75litre per second and rotational speed of 350 rpm. Table 4.11 contained the values of shaft power and efficiency.

Figure 16 shows the Performance curves of the turbine by variation of the blade entry/ exit angle.

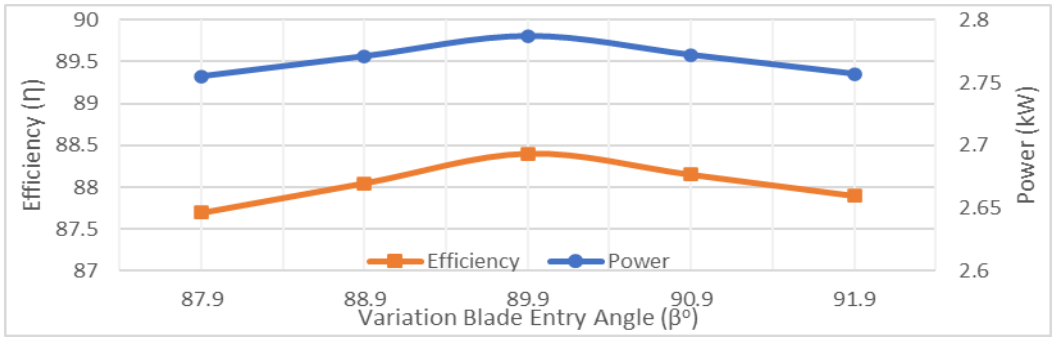

Fig. 16: Performance characteristics of optimized turbine with varying blade entry/ exit angles

Varying the inlet/ exit angle increased the power output by 30W and an efficiency increase of 0.5%. The marginal increased in efficiency was also observed by Choi *et al.* (2008) and Tiwari *et al.* (2017).

Casing optimization

The length of the casing tip (where the nozzle tip merged casing) was varied between 30mm and 100mm (the base design being 40mm), their performances were simulated using the optimized flow rate of 75 litre per second and rotational speed of 350 rpm. Table 4.12 contained the values of shaft power and efficiency and Figure 4.34 shows the

Performance curves of the turbine by variation of the casing length tip. Optimization of the casing tip length improved by 1.7% and 40 watts in efficiency brake horsepower respectively. N. Acharya *et al.* (2015) made similar observation.

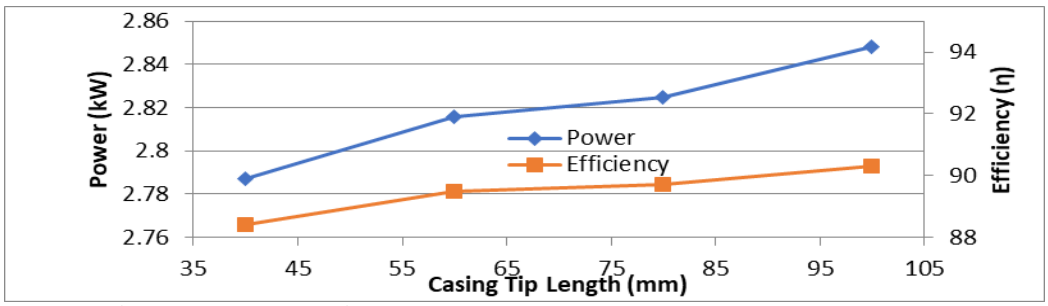

Fig. 17: Performance characteristics of optimized turbine at varying casing tip length

Figure 18 shows the comparison of velocity contours of the turbine by extending the casing tip length from 40mm to 100mm.

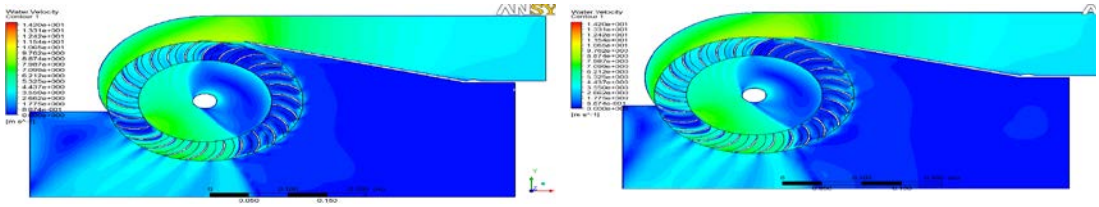

Figure 18: Comparison between Base Design of Casing and F100 Casing @ 75L

Summary

The research work focuses on the optimization of flow through a simple crossflow turbine with commercial software ANSYS CFX, thereby improving its efficiency. The work also identified a simplified method of construction and use of readily available materials in the local market for the construction of the turbine. A test facility was designed and constructed for the manufactured turbine and performance test carried out at different hydraulic heads, flow rate, rpm and gate openings.

Findings and discoveries made while carrying out the research are as follows:

1. The use of pipe strips as runner blade is viable provided that the right diameter, inlet/outlet angle orientation, diameter ratio and number of blades are correctly determined. In this case, pipe diameter of 72mm, inlet angle of 28^o and outlet of 92^o, diameter ratio of 0.69 and 26 blades gives the highest efficiency with an improvement of 7.1% above the base case.
2. The nozzle shape modification of crossflow turbine improves the efficiency the most. An improvement of 7.9% was obtained by tinkering with angle of attack, extending the admission arc by 10^o and the width to that of the runner.
3. The Casing tip extension by about 60mm free the exiting water thereby improving the efficiency by 1.9%.
4. The result of simulation performed with K-Epsilon model compares well with that done with SST model.

Reference

Acharya, N., Kim, C.-G., Thapa, B., & Lee, Y.-H. J. R. e. (2015). Numerical analysis and performance enhancement of a cross-flow hydro turbine. *80*, 819-826.

Acharya, R. (2016). Investigation of differences in Ansys solvers CFX and fluent. In.

Adanta, D., Hindami, R., & Siswantara, A. I. (2018). *Blade depth investigation on cross-flow turbine by numerical method*. Paper presented at the 2018 4th International Conference on Science and Technology (ICST).

Adanta, D., Warjito, B., Prakoso, A. P., & Wijaya, E. P. J. C. L. (2019). Effect of Blade Depth on the Energy Conversion Process in Crossflow Turbines. *12*(1), 123-131.

Adhikari, R. (2016). Design improvement of crossflow hydro turbine.

Adhikari, R., & Wood, D. J. E. (2018). The design of high efficiency crossflow hydro turbines: A review and extension. *11*(2), 267.

Anderson, J. D., Degrez, G., Dick, E., & Grundmann, R. (2013). *Computational fluid dynamics: an introduction*: Springer Science & Business Media.

Benišek, M., Čantrak, S., Nedeljković, M., Ilić, D., Božić, I., & Čantrak, Đ. J. F. T. (2005). Defining the optimum shape of the cross-flow turbine semi-spiral case by the lagrange's principle of virtual work. *33*(3), 141-144.

Bijukchhe, V. (2012). Comparison of experimental results of horizontal kaplan turbine with computational fluid dynamics.

Ceballos, Y. C., Valencia, M. C., Zuluaga, D. H., Del Rio, J. S., & García, S. J. I. J. O. R. E. R. I. (2017). Influence of the number of blades in the power generated by a Michell Banki Turbine. *7*(4).

Choi, Y.-D., Lim, J.-I., Kim, Y.-T., Lee, Y.-H. J. J. o. f. s., & technology. (2008). Performance and internal flow characteristics of a cross-flow hydro turbine by the shapes of nozzle and runner blade. *3*(3), 398-409.

Choi, Y.-D., & Son, S.-W. J. 한. (2012). Shape effect of inlet nozzle and draft tube on the performance and internal flow of cross-flow hydro turbine. *36*(3), 351-357.

Dametew, A. W. J. G. J. o. R. I. E. (2016). Design and Analysis of Small Hydro Power for Rural Electrification.

Desai, V. R., & Aziz, N. M. (1994). An experimental investigation of cross-flow turbine efficiency.

Fukutomi, J., Nakase, Y., Ichimiya, M., Ebisu, H. J. J. I. J. S. B. F., & Engineering, T. (1995). Unsteady fluid forces on a blade in a cross-flow turbine. *38*(3), 404-410.

Gu, X., Yin, J., Liu, J., & Wu, Y. J. M. P. i. E. (2014). A Nonlinear k-Turbulence Model Applicable to High Pressure Gradient and Large Curvature Flow. *2014*.

Hu, H. H. (2012). Computational fluid dynamics. In *Fluid mechanics* (pp. 421-472): Elsevier.

Iovănel, R., Bucur, D.-M., & Cervantes, M. J. J. o. A. F. M. (2019). Study on the Accuracy of RANS Modelling of the Turbulent Flow Developed in a Kaplan Turbine Operated at BEP. Part 1-Velocity Field. *12*(5), 1449-1461.

Joshi, C., Seshadri, V., & Singh, S. (1995). Modifications in a cross flow turbine for performance improvement.

Khare, R., Prasad, V. P., Kumar, S. J. H. N. J. o. W., Energy, & Environment. (2010). Derivation of Global Parametric Performance of Mixed Flow Hydraulic Turbine Using CFD. *7*, 60-64.

Khosrowpanah, S., Fiuzat, A., & Albertson, M. L. J. J. o. H. E. (1988). Experimental study of cross-flow turbine. *114*(3), 299-314.

Mani, S., Shukla, P. K., & Parashar, C. J. I. J. o. E. S. (2016). Effect of Changing Number of Blades and Discharge on the Performance of a Cross-Flow Turbine for Micro Hydro Power Plants. *2957*.

Menter, F., Ferreira, J. C., Esch, T., Konno, B., & Germany, A. (2003). *The SST turbulence model with improved wall treatment for heat transfer predictions in gas turbines.* Paper presented at the Proceedings of the international gas turbine congress.

Mockmore, C. A., & Merryfield, F. (1949). The Banki water turbine.

Nakase, Y. (1982). *A study of cross-flow turbine (effects of nozzle shape on its performance).* Paper presented at the ASME 103rd Winter Annual Meeting.

Olgun, H. J. I. j. o. e. r. (1998). Investigation of the performance of a cross-flow turbine. *22*(11), 953-964.

Oliy, G. B., Ramayya, A. V. J. I. J. o. S., Technology, & Society. (2017). Design and Computational Fluid Dynamic Simulation Study of High Efficiency Cross Flow Hydro-power Turbine. *5*(4), 120-125.

Orso, R., Benini, E., Minozzo, M., Bergamin, R., & Magrini, A. J. E. (2020). Two-Objective Optimization of a Kaplan Turbine Draft Tube Using a Response Surface Methodology. *13*(18), 4899.

Peláez Restrepo, J. D. (2014). *Study of the effect of the geometrical parameters of the runner and operation conditions on performance and flow characteristics in a cross flow turbine.* Universidad EAFIT,

Pereira, N. C., & Borges, J. J. I. j. o. m. s. (1996). Study of the nozzle flow in a cross-flow turbine. *38*(3), 283-302.

Pereira, N. H., & Borges, J. (2014). *A study on the efficiency of a cross-flow turbine based on experimental measurements.* Paper presented at the Proceedings of the 5th International Conference on Fluid Mechanics and Heat & Mass Transfer (FLUIDSHEAT'14), Lisbon, Portugal.

Pokhrel, S. (2017). *Computational Modeling of A Williams Cross Flow Turbine.* Wright State University,

Sammartano, V., Aricò, C., Carravetta, A., Fecarotta, O., & Tucciarelli, T. J. E. (2013). Banki-Michell optimal design by computational fluid dynamics testing and hydrodynamic analysis. *6*(5), 2362-2385.

Soenoko, R. J. I. J. o. A. E. R. (2016). First stage cross flow turbine performance. *11*(2), 938-943.

Sutikno, D., Soenoko, R., Soeparman, S., Wahyudi, S., & Azmi, M. A. (2019). The performance characteristics of the low head cross flow turbine using nozzle roof curvature radius centered on shaft axis. *%J International Journal of Integrated Engineering*, *11*(5), 12-22.

Sutikno, D., Soenoko, R., Soeparman, S., & Wahyudi, S. J. B.-E. ж. п. т. (2019). Flow visualization of water jet passing through the empty space of cross-flow turbine runner. (3 (8)), 36-42.

Tiwari, M., & Shrestha, R. J. J. o. t. I. o. E. (2017). Effect of variation of design parameters on cross flow turbine efficiency using ANSYS. *13*(1), 1-9.

Tongco, A. F. (1988). *Field testing of a crossflow water turbine.* Oklahoma State University,

Totapally, H. G., & Aziz, N. M. J. J. o. e. e. (1994). Refinement of cross-flow turbine design parameters. *120*(3), 133-147.

Walseth, E. C. (2009). *Investigation of the Flow through the Runner of a Cross-Flow Turbine.* Institutt for energi-og prosessteknikk,